

Analysis of Sumatran Earthquake Coulomb Stress Changes in Geothermal Potential in Rianite, Samosir Regency

Goldberd Harmuda Duva Sinaga* & Juliper Nainggolan

Physics Education Study Program, Universitas HKBP Nommensen, Indonesia

*Corresponding Author: goldberhdhsinaga@gmail.com

Received: 20 October 2023; Accepted: 30 November 2023; Published: 13 December 2023

DOI: <https://dx.doi.org/10.29303/jpft.v9i2.5900>

Abstract - Increasing energy demand and high world oil prices are making countries turn to geothermal energy use. Indonesia is a country that has geothermal energy due to Indonesia's geographical location and geological conditions, which is located between three active earth plates so that Indonesia has 240 volcanoes and often experiences earthquakes. The 2003-2013 earthquake data obtained are coordinates, magnitude, depth, focal mechanism and all these data are analyzed in the coulomb stress method. Rianiate geothermal measurement data in March 2013 included geothermal location, hot spring and air temperature, pH, and geochemical measurements. The analysis results showed that the highest coulomb stress value was at a depth of 90 km of 0.56 bar while the shear and normal values were 0.452 bar and 0.251 bar. The result of the spread of coulomb stress is to the northeast, east and southeast. Then the results of the analysis of the direction of distribution of coulomb stress are compared to the location of the hot spring based on a decrease in temperature, the change in the potential of hot spring 1 leads to hot spring 2, 3, and 4 in the opposite direction, namely northwest or leads to the largest source of coulomb stress, so that Coulomb Stress Changes affect indirectly changes in the geothermal potential of Rianiate.

Keywords: Earthquake; Coulomb Stress; Geothermal

INTRODUCTION

Energy needs continue to increase and high world oil prices make countries in the world reduce their dependence on oil by switching to the use of renewable energy. The development of renewable energy resources into a renewable energy industry aims to reduce dependence on fossil fuels and greenhouse gas emissions by developing renewable energy power plants (Sutriani & Wijayanto, 2020) (Fefria Tanbar, 2022) (Cahyono et al., 2019) (Fandari, 2014).

Indonesia has the potential of renewable energy sources. This can be seen from the geographical location and geological conditions of Indonesia, which is located between three active earth plates, the Pacific plate, the Indo-Australian plate and the Eurasian plate. Active plates mean that they are always moving and interacting with each other. The Pacific plate moves relatively to the West, the Indo-Australian plate moves relatively to the north and the

Eurasian plate moves relatively to the southeast

Indonesia has approximately 240 volcanoes, of which almost 70 are still active (Soares, 2013), so that it is included in the active mountain range in the world (ring of fire), which is spread from west to east of Indonesia (Suharmanto et al., 2015). In addition, Indonesia is also on the path of The Pacific Ring of Fire. The Pacific Ring of Fire runs between the subduction and separation of the Pacific plate from the Indo-Australian plate, the Eurasian plate, the North American plate and the Nazca plate colliding with the South American plate (Soares, 2013) (Baksir et al., 2019)

In the earth's crust, a source of thermal energy called geothermal energy is formed. In a geothermal system, this energy is contained in water vapor, hot water, and rocks, as well as other gases and minerals that cannot be separated (Fandari, 2014) (Lestari et al., 2019). Geothermal is

one example of renewable energy that can be used as a power plant by minimizing adverse impacts on the environment (Umam et al., 2018).

Based on the tectonics of Sumatra Island, the geothermal system of Siogung-ogung area, Samosir Regency is closely related to the horizontal fault structure (dextral) of Sumatra and the magmatic path (magmatic arc) stretching from Sumatra, Java, Bali, West Nusa Tenggara, Flores Islands to North Sulawesi. Toba Caldera and G. Pusuk Bukit are part of many volcanic phenomena in Sumatra with a volcanic hydrothermal system model (Henley, 1995)(N. Ninggolan et al., 2018). The geological structure in the Geothermal Field in the Siogung-ogung area is in the form of a horizontal fault in the Northwest-Southeast direction.

Northern Sumatra is an area prone to earthquakes due to the collision activity of the Indo-Australian and Eurasian plates. The fault that occurs in North Sumatra is influenced by several active segments, one of which is several active tectonic earthquake segments one of them is located in Renun which stretches from North Tapanuli to Sidikalang (Wulandari et al., 2021)

The relationship between earthquakes and earthquake activity can be seen through Coulomb Stress Changes. Several cases of earthquake relations with volcanic activity occur in several volcanoes in Indonesia and outside Indonesia (Kototabang & Geofisika, 2013)(Sinaga et al., 2022). The results of the analysis of coulomb stress changes on Mount Sinabung resulted in earthquakes that occurred in Sumatra affecting Sinabung volcanic activity with a coulomb stress value of 0.118 bar in 2016 (Goldberd Harmuda Duva Sinaga, Winarto Silaban, et al., 2022). In addition to increasing stress around Mount Sinabung, earthquakes that occur in

Sumatra also affect pyroclastic flows where the direction of positive stress is opposite to the direction of pyroclastic flow. (Goldberd Harmuda Duva Sinaga, Switamy Angnitha Purba, et al., 2022). The same case also occurred on Mount Sorikmarapi and Mount Rinjani, Mount Merapi, Mount Soputan and Gamalama (Sinaga et al., 2021)(Utama et al., 2020) (Walter et al., 2007)(Sinaga et al., 2017). Thus, the phenomenon of earthquakes that occur against volcanic activity needs to be done research on coulomb stress analysis on geothermal in Rianiate Samosir.

RESEARCH METHODS

The method used in research on Mount Sibayak is the analytical-descriptive method. The model used in this study is the Coulomb Stress Model. Earthquake data were obtained from Global CMT, Geofon, and IRIS Concorium. Earthquake stress/strain will be analyzed in coulomb 3.3 software. The value and distribution of stress/strain from the earthquake will be mapped in 2D and 3D using Global Mapping Tool Software and Google Earth Software. The data used in this study are earthquake magnitude and coordinate data, earthquake depth, earthquake type (strike, slip, dip), and moment tensor (Shinji Toda, Ross S. Stein, Volkan Sevilgen, 2011). Although many earthquakes occurred in northern Sumatra, only those analyzed had focal mechanisms.

By considering the failure of the fracture as the cause of the combined normal (minimized) and shear stress conditions, it is measured as the criterion of static coulomb stress (King et al., 1994) Changes in static coulomb stress caused by earthquakes can help explain the distribution of aftershocks (Parsons et al., 1999), because aftershocks will occur at any time when the coulomb stress exceeds the shear strength of the fault

surface. The state coulomb stress change (ΔCFF) defines as

$$\Delta CFF = \Delta\tau + \mu (\Delta\sigma + \Delta p) \quad (1)$$

$\Delta\tau$ represents the change in shear stress at fault (positive in the slip direction), $\Delta\sigma$ is the change in normal stress (positive for an uncompressed fracture), Δp is the change in pore pressure, and μ is the coefficient of friction, which ranges from 0.6 to 0.8 for most intact rocks (Harris, 1998). In Oklahoma, where the fluid injection was 1-2 km deep near the epicentre, this has been used for disposal since 1993 (Keranen et al., 2013). In addition, the effect of pore pressure cannot be ignored. The change in pore pressure after a change in stress occurs and there is no fluid flow (undrained condition) is

$$\Delta p = \frac{\beta \Delta \sigma_{kk}}{3} \quad (2)$$

where β is Skempton's coefficient, and σ_{kk} is the number of diagonal elements of the stress tensor (Rice, 1992). The Skempton coefficient describes the change in pore pressure resulting from a change in externally applied stress and often ranges in value from 0.5 to 1.0. (Green & Wang, 1986)(Hart & Wang, 1995)(Cocco, 2002). For fault zone rheology, where the fracture zone material is more rigid than the surrounding material, $\sigma_{xx} = \sigma_{yy} = \sigma_{zz}$ (Rice, 1992)(Simpson, 1992)(Harris, 1998); so, $\frac{\Delta \sigma_{kk}}{3} = \Delta \sigma$. Equation (1) and (2) combined with this assumption, create

$$\Delta CFF = \Delta\tau + \mu' \Delta\sigma \quad (3)$$

Where $\mu' = \mu (1 - \beta)$, Effective friction coefficient. The effective coefficient of friction generally ranges from 0.0 to 0.8, but it is usually around 0.4 ($\mu = 0,75, \beta = 0,47$) For horizontal faults or faults whose

orientation is unknown (Parsons et al., 1999). These values are typically used in the calculation of Coulomb Stress Changes to minimize uncertainty. The location and geometry of the fault source, as well as the division of slip over the plane source, play an important role in calculating coulomb stress changes. Based on earthquake magnitude, we model the source geometry with empirical relationships for strike-slip errors (Wells, Donald L. Coppersmith, 1994), which was built into Coulomb Software 3.3 (Shinji Toda, Ross S. Stein, Volkan Sevilgen, 2011).

After the earthquake is analyzed in the coulomb stress method, the next step is the collection of geothermal data Rianiate Samosir in the form of location and investigation of geophysical principles and investigation of geochemical principles of hot eyes from geothermal. Data geothermal Rianiate Samosir. Data from geophysical investigations include air temperature and spring temperature. While data from geochemical investigations include levels HCO_3 , SO_4 , Cl, Na, K, and dan Magnesium. The results of this study were taken from one of the results of geothermal research by Juliper Nainggolan in 2013 (Nainggolan et al., 2017)(*Determining Potential and Model of Rianiate Geothermal*, 2017). Geothermal data collection was caused by an earthquake that occurred in the waters of Lake Toba / Mount Toba a few months before this geothermal research was carried out

After taking this geothermal data is done, the next step is analysis with the description method and also displayed in the form of a map (google earth) so that it can produce answers about changes in geothermal potential due to coulomb stress analysis from earthquakes that occur.

RESULTS AND DISCUSSION

Results

In this study, the Δ CFS model was used to determine the distribution of static stress by the Sumatra earthquake. Modeling Δ CFS It is also used to determine the relationship of earthquakes to aftershocks, as well as the relationship between tectonic and volcanic earthquakes; (Utama et al., 2020).

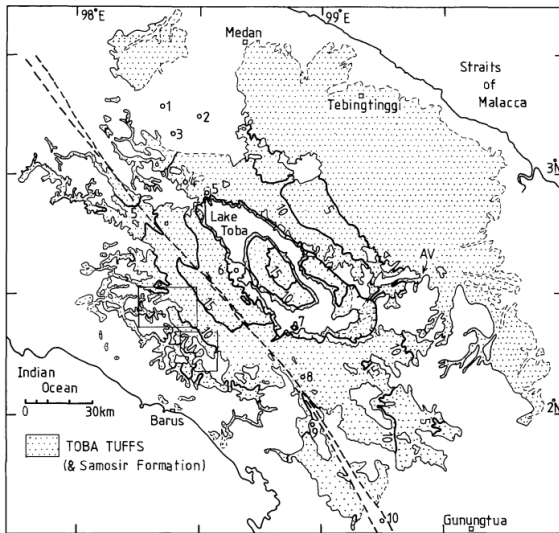


Figure 1. The topographic boundary of Toba depression is indicated by a thick line with ticks in it, equivalent to contours of 1500 m and 1000 m. small circles mark the Quaternary volcanic center: 1, Bekulap; 2, Sibayak; 3, Sinabung; 4, Artificial; 5, Horn continent; 6, Pusukbukit; 7, Pardepur; 8, Immune; 9, Martimban; 10, Warden. Image location. 4 outlined. AV: Asahan Valley (Aldiss & Ghazali, 1984)

Since the Aceh earthquake, December 26, 2004, the area around Sumatra Island, especially the northern part, is very vulnerable to earthquakes. Several researchers have evaluated changes in subduction zone stress, in the Sumatran fault, especially the 13 active volcanoes on the Sumatran mainland. We have found that earthquakes that have occurred since 2004 have changed stress across subduction tectonic regions (Qiu & Chan, 2019). Great Sumatra Fault (GSF) is one of the active faults that is always monitored. The high value of instability, makes it more susceptible to slip movements, stress

buildup, to the occurrence of fault collapses (earthquakes) in later periods (Kusumawati et al., 2021)(Hardebeck & Okada, 2018). Figure 1 shows the topographic boundary of Toba depression marked by a thick line with a tick in it, equivalent to the contours of 1500 m and 1000 m with Mount Toba / Lake Toba shown in number 6. (Aldiss & Ghazali, 1984).

Coulomb Stress Changes in 2003-2013 in North Sumatra and Nias

The results of coulomb stress changes that occurred in North Sumatra and Nias came from the analysis of 112 earthquake events that occurred in North Sumatra and Nias from March 2003 – March 2013. Table 1 displays the results of the analysis of 112 earthquake events that also produce a higher stress value, which is a depth of 40 km and below. This is due to earthquakes that occurred in North Sumatra and West Nias on average at a depth of 50 km.

Table 1. Coulomb Stress Change in Rianiate and Nias

Number	Depth (km)	Shear (bar)	Normal (bar)	Coulomb (bar)
1	0.00	-0.387	0.388	-0.232
2	10	-0.349	0.131	-0.296
3	20	-0.249	-0.01	-0.253
4	30	-0.11	-0.054	-0.132
5	40	0.045	-0.024	0.035
6	50	0.194	0.051	0.215
7	60	0.319	0.138	0.374
8	70	0.406	0.209	0.49
9	80	0.452	0.248	0.551
10	90	0.46	0.251	0.56
11	100	0.438	0.221	0.526
12	110	0.396	0.17	0.464
13	120	0.343	0.107	0.385
\bar{x}		0.150	0.140	0.206

Temperature and geochemical measurements of the Rianiate Hot Springs

The research conducted in Rianiate Village, Pangururan sub-district which administratively under governance of Samosir Regency. Geographically, this area is located at position 98°42'– 98°47' East Longitude and 2°32' - 2°45' North latitude. This location has an area of 121.43 km², with the boundaries of the region is as follows. North side is Simanindo Sub-district, South side is District Palipi, West side is Sianjur Mulamula District, and East is Ronggur Nihuta District. (Nainggolan et al., 2017)(*Determining Potential and Model of Rianiate Geothermal*, 2017).

Table 2. Location Hot Spring and Temperature

Hot Spring	Coordinate		Height meter	Air Temp. °C	Water Temp. °C
	lat	Lon			
1	02°31	98°44	958	26	43
2	02°31	98°44	946	26	77
3	02°31	98°44	977	26.5	79
4	02°31	98°44	980	27	80

The hot springs in terms their specific geological location, physical as well as chemical properties. The four springs identified as spring 1, spring 2, spring 3, and spring4 (Table 2).

Table 3. The chloride, sulfate, and bicarbonate ion content of various spring

Hot Spring	pH	The chloride, sulfate, and bicarbonate ion content of various spring.		
		HCO ₃	SO ₄	Cl
1	6.2	0	43.6	95.63
2	6.3	0	7.18	92.81
3	6.5	0	10.02	89.97
4	6.4	38.71	7.45	53.82

To determine types of hot water, we calculated the ion content in meq/L, the result was compared using trilinear classification diagram. Based on the percentage of ion content in hot water samples which have been analyzed chemical

element content especially Biocarbonate anion content (HCO₃-), Clorida (Cl⁻), and Sulfate (SO₄) that be determined through Water type (Table 3).

Table 4. Elemental ratio of Na/1000, K/100, and Mg

Hot Spring	The chloride, sulfate, and bicarbonate ion content of various spring.		
	N/1000	K/1000	Mg/1000
1	0.00084	0.001	0.52
2	0.0879	0.2189	0.89
3	0.02978	0.1711	0.94
4	0.0886	0.001	0.74

The water type was determined by using triangle diagram, generally the water under inspection is in the immature waters area. Although the composition of the most dominant ionic ratio of Na/1000 – K/100 - Mg relatively difference, the global type are similar. It means that the hot water springs has contaminated by surface water.(Table 4.)(Nainggolan et al., 2017)(*Determining Potential and Model of Rianiate Geothermal*, 2017).

Discussion

Coulomb Stress Changes in 2003-2013 in North Sumatra and Nias

The modeling of ΔCFS performed to determine the static stress distribution of earthquakes. In addition, this method can also be used to see the relationship between earthquakes that can trigger subsequent earthquakes, both between major earthquakes and aftershocks, and the relationship between tectonics and volcanic earthquakes. The positive value lobes are marked in red which is an area of increased coulomb stress of 0-5 bar. While the negative lobe is marked in blue which is an area of decrease in coulomb stress 0-5 bar. (Utama et al., 2020). The positive value

lobes are marked in red which is an area of increased coulomb stress of 0-5 bar. While the negative lobe is marked in blue which is an area of decrease in coulomb stress 0-5 bar.

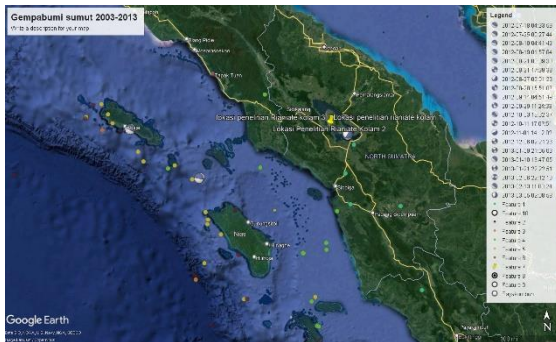


Figure 2. The spread of earthquakes that occurred in North Sumatra and Nias from 2003-2013

The earthquake that occurred in Lake Toba and surrounding Tapanuli from March 2003 to March 2013, resulted in a coulomb stress distribution under Rianiate. Figure 2 shows the spread of coulomb stress towards the north, northeast, and east. This depends on the combination of earthquakes in North Sumatra and Nias Island. The magnitude of coulomb stress changes varies at depth.

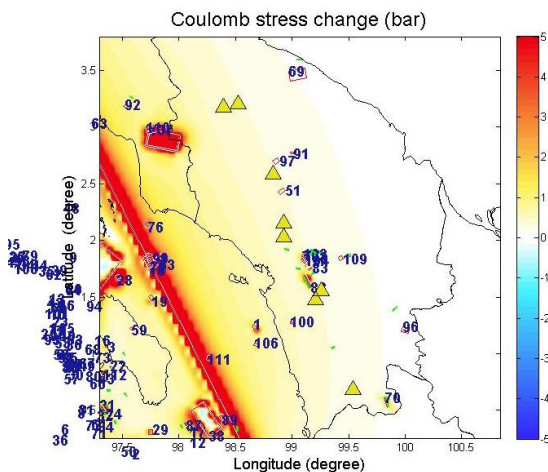


Figure 3. Coulomb Stress Changes Earthquakes in North Sumatra and Nias in 2003-2013

The results of coulomb stress analysis in Rianiate resulted in the lowest shear value being at 0 km at -0.387 bar while the highest shear value was at a depth of 90 km at 0.46 bar. The lowest normal value is at a depth of

20 km of -0.01 bar and the highest normal value is at a depth of 0 km of 0.388 bar. The highest coulomb stress change was at a depth of 90 km at 0.56 bar while the lowest coulomb value was at a depth of 30 km at -0.132 bar. This value indicates that the surface of the Rianiate area experiences strains starting from a depth of 0-30 km and after that Rianiate experiences stress up to a depth of 120 km. But overall Rianiate has an average shear value of 0.150 bar, normal, 0.140 bar and coulomb of 0.206 bar.

From table 1, the coulomb stress change value drops again after 100 km. This is because the number of earthquakes that occur at depths of more than 150 km is rare like the earthquake that occurred on August 27, 2012. Earthquakes that occur in the waters of Lake Toba (Mount Toba) have an average depth below 150 km.

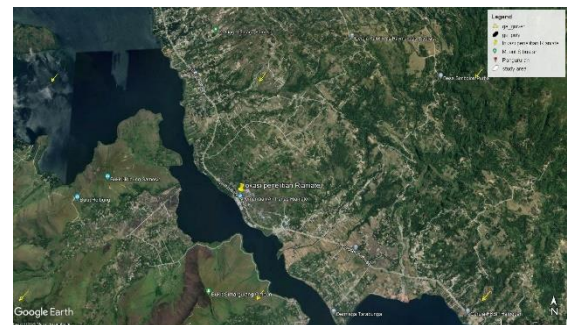


Figure 4. Direction of source of distribution of coulomb stress in Geothermal Rianiate in 2003-2013

However, after the earthquake that occurred on August 27, 2012, Lake Toba experienced an increase in the intensity of earthquake events compared to before, so researchers can argue that Lake Toba will experience more frequent earthquake intensity as earthquakes increase on the west coast, Nias, and surrounding areas. This is due to coulomb stress values that increase over time. The source of the distribution of coulomb stress changes in the Geothermal Rianiate points southwest according to the number of earthquakes that occur. This distribution can be seen from figure 4.

Analysis of Coulomb Stress Changes on Samosir Geothermal Rianiate

The results of Rianiate geothermal research in Tables 2, 3, and 4 were obtained from Juliper Nainggolan's research which in his research included geothermal and geophysical Rianiate on March 13, 2013 where this research was also carried out at a time not too far from the earthquake that occurred August 27, 2012.

If you look at the position of the pool/hot spring based on coordinates, then hot spring no. 4 is in the highest position and is the easternmost followed by the pool to the west, namely pools 3, 1, and 2. If you look at the table, the physical property is that the air temperature will be lower if it is going west (Table 2). Likewise, the temperature of the hot water is also smaller if the pool is heading westward. But for pH is in the west pool (pools 3, 2, and 1).

It depends on the geological conditions of the rock that affect the pH of the hot water. However, physical properties and pH differ from chloride, sulfate, and bicarbonate measurements. Only pool 4 had HCO_3 while SO_4 concentrations were in pools 3, 2, and 1 with pools 4 and 2 having almost the same measurement values (Table 3). For the highest Cl measurement, the west pool is pool 1, 2, and 3. This also applies to potassium measurements that have the highest values in pools 1, 2, and 3. Magnesium measurements were highest in pools 3, 2, 4, and 1. The difference in chemical properties of HCO_3 , SO_4 , Cl, N, K, and Mg is determined by the geological properties of the rocks in the pond, while the physical properties of air temperature and hot water temperature that have the highest value to the lowest value can be seen from the location successively east to west (southwest) (Table 4)

The direction of this highest value is similar to the direction of distribution of coulomb stress, which is east to southwest. From the similarity of this phenomenon, it can indicate the influence of earthquakes and coulomb stress distribution on changes in the geothermal potential of Rianiate Samosir, although further research is needed on this relationship. This study is also almost similar to previous studies where the direction of coulomb stress distribution affects the direction of pyroclastic flow of Mount Sinabung (Goldberd Harmuda Duva Sinaga, Winarto Silaban, et al., 2022).

CONCLUSION

Earthquakes that occur in North Sumatra, especially the west coast and Nias, indirectly affect the geothermal potential, namely a decrease in air temperature and hot water temperature, where the source of the direction of distribution of coulomb stress comes from east to west (southwest), as well as the direction of decreasing air temperature and decreasing hot water temperature towards the east.

ACKNOWLEDGMENT

Researchers are grateful to the research data providers, namely Global CMT, IRIS, Geofon, and also to Juliper Nainggolan for the Geothermal data provided.

REFERENCES

- Aldiss, D. T., & Ghazali, S. A. (1984). The regional geology and evolution of the Toba volcano-tectonic depression, Indonesia. *Journal of the Geological Society*, 141(3), 487–500. <https://doi.org/10.1144/gsjgs.141.3.0487>
- Baksir, A., Daud, K., Wibowo, E. S., Akbar, N., & Haji, I. (2019). Pemanfaatan Sumber Energi Panas Bumi Untuk Pengeringan Ikan Di Desa Idamdehe

- Kabupaten Halmahera Barat Provinsi Maluku Utara. *Jphi*, 22(3), 423–432.
- Cahyono, B. E., Jannah, N., & Suprianto, A. (2019). Analisis Sebaran Potensi dan Manifestasi Panas Bumi Pegunungan Ijen Berdasarkan Suhu Permukaan dan Geomorfologi. *Natural B*, 5(1), 19–27.
- Cocco, M. (2002). Pore pressure and poroelasticity effects in Coulomb stress analysis of earthquake interactions. *Journal of Geophysical Research*, 107(B2). <https://doi.org/10.1029/2000jb000138>
- Determining Potential and Model of Rianiate Geothermal*. (2017). 5(6), 145–150.
- Fandari, N. E. L. (2014). *Pengembangan Energi Panas Bumi yang Berkelanjutan*. 17(1), 68–82.
- Fefria Tanbar, A. A. S. I. A. A. (2022). Studi Perhitungan Potensi Cadangan Panas Bumi Pada Lapangan Jailolo Di Wilayah Halmahera. *Jurnal Offshore: Oil, Production Facilities and Renewable Energy*, 6(1), 14–20.
- Goldberd Harmuda Duva Sinaga, Switamy Angnitha Purba, & Ady Frenly Simanullang. (2022). Coulomb Stress Analysis And Monte Carlo Simulation In Predicting Sinabung Pyroclastic Flow. *World Journal of Advanced Research and Reviews*, 13(1), 781–792. <https://doi.org/10.30574/wjarr.2022.13.1.0085>
- Goldberd Harmuda Duva Sinaga, Winarto Silaban, & Ady Frenly Simanullang. (2022). Analysis of Coulomb Stress of Sumatera Earthquake Against Pyroclastic Flow of Mount Sinabung as Data Prone Volcano Disaster. *World Journal of Advanced Research and Reviews*, 13(1), 793–803. <https://doi.org/10.30574/wjarr.2022.13.1.0086>
- Green, D. H., & Wang, H. F. (1986). *ap*. 51(4), 948–956.
- Hardebeck, J. L., & Okada, T. (2018). Temporal Stress Changes Caused by Earthquakes: A Review. *Journal of Geophysical Research: Solid Earth*, 123(2), 1350–1365. <https://doi.org/10.1002/2017JB014617>
- Harris, R. A. (1998). Introduction to special section: Stress triggers, stress shadows, and implications for seismic hazard. *Journal of Geophysical Research: Solid Earth*, 103(10), 24347–24358. <https://doi.org/10.1029/98jb01576>
- Hart, D. J., & Wang, H. F. (1995). limestone of the pore $E = \text{all } K \cdot$. *Journal of Geophysical Research: Solid Earth*, 100(95), 741–751.
- Henley, R. W. (1995). Geothermal fluids: Chemistry and exploration techniques. In *Journal of Geochemical Exploration* (Vol. 52, Issue 3). [https://doi.org/10.1016/0375-6742\(95\)90013-6](https://doi.org/10.1016/0375-6742(95)90013-6)
- Keranen, K. M., Savage, H. M., Abers, G. A., & Cochran, E. S. (2013). Potentially induced earthquakes in Oklahoma, USA: Links between wastewater injection and the 2011 Mw 5.7 earthquake sequence. *Geology*, 41(6), 699–702. <https://doi.org/10.1130/G34045.1>
- King, G. C. P., Stein, R. S., & Jian Lin. (1994). Static stress changes and the triggering of earthquakes. *Bulletin - Seismological Society of America*, 84(3), 935–953. [https://doi.org/10.1016/0148-9062\(95\)94484-2](https://doi.org/10.1016/0148-9062(95)94484-2)
- Kototabang, S. P. A. G. (GAW) B., & Geofisika, B. M. K. dan. (2013). HUBUNGAN ANTARA GEMPABUMI DENGAN ERUPSI GUNUNGAPI STUDI KASUS ERUPSI GUNUNG SINABUNG TAHUN 2010 DAN 2013. *Megasains*, 4(Desember 2013), 117 – 123.
- Kusumawati, D., Sahara, D. P., Widiyantoro, S., Nugraha, A. D., & Muzli, M. (2021). *Fault Instability and*

- Its Relation to Static Coulomb Failure Stress Change in the 2016 Mw 6.5 Pidie Jaya Earthquake, Aceh, Indonesia.* 8(February), 1–13. <https://doi.org/10.3389/feart.2020.559434>
- Lestari, E. Y., Sumarto, S., & Artikel, I. (2019). Indonesian Journal of Conservation. *Indonesian Journal of Conservation*, 8(01), 93–102. <https://doi.org/10.15294/ijc.v11i2.40599>
- N. Ninggolan, E., Ekklesia, S., & Kiswiranti, D. (2018). Identifikasi Potensi dan Sistem Panas Bumi Daerah Di Ogung-Ogung, Samosir, Sumatera Utara. *Seminar Nasional Kebumihan Ke-11*, 1075–1084. <https://repository.ugm.ac.id/274916>
- Nainggolan, J., Sitepu, C., Pardede, S., & Diantoro, M. (2017). Geohydrology, geochemistry, geothermal potency of Rianiate Toba Lake North Sumatera. *IOP Conference Series: Materials Science and Engineering*, 237(1). <https://doi.org/10.1088/1757-899X/237/1/012007>
- Parsons, T., Stein, R. S., Simpson, R. W., & Reasenber, P. A. (1999). Stress sensitivity of fault seismicity: A comparison between limited-offset oblique and major strike-slip faults. *Journal of Geophysical Research: Solid Earth*, 104(B9), 20183–20202. <https://doi.org/10.1029/1999jb900056>
- Qiu, Q., & Chan, C. (2019). Journal of Asian Earth Sciences Coulomb stress perturbation after great earthquakes in the Sumatran subduction zone: Potential impacts in the surrounding region. *Journal of Asian Earth Sciences*, 180(May), 103869. <https://doi.org/10.1016/j.jseaes.2019.103869>
- Rice, J. R. (1992). Fault Stress States, Pore Pressure Distributions, and the Weakness of the San Andreas Fault. *International Geophysics*, 51(C), 475–503. [https://doi.org/10.1016/S0074-6142\(08\)62835-1](https://doi.org/10.1016/S0074-6142(08)62835-1)
- Shinji Toda, Ross S. Stein, Volkan Sevilgen, and J. L. (2011). *Coulomb 3.3 Graphic-Rich Deformation and Stress-Change Software for Earthquake, Tectonic, and Volcano Research and Teaching—User Guide*. U.S. Geological Survey, Reston, Virginia: 2011. <https://www.usgs.gov/software/coulomb-3>
- Simpson, W. (1992). *Response of Regional Seismicity*. 6, 1687–1690.
- Sinaga, G. H. D., Loeqman, A., Siagian, R. C., & Sinaga, M. P. (2022). Analysis of Coulomb Stress Changes in Aceh Earthquake on Sibayak Volcano. *Jurnal Pendidikan Fisika Dan Teknologi*, 8(2), 217–227. <https://doi.org/10.29303/jpft.v8i2.4409>
- Sinaga, G. H. D., Tambunan, M. R., Loeqman, A., & Wibowo, A. (2021). Coulomb Stress Change of the 2004 Aceh Earthquake on Mount Sorik Marapi 2021. *Jurnal Penelitian Fisika Dan Aplikasinya (JPFA)*, 11(2), 158–170. <https://doi.org/10.26740/jpfa.v11n2.p158-170>
- Sinaga, G. H. D., Zarlis, M., Sitepu, M., Prasetyo, R. A., & Simanullang, A. (2017). Coulomb stress analysis of West Halmahera earthquake mw=7.2 to mount Soputan and Gamalama volcanic activities. *IOP Conference Series: Earth and Environmental Science*, 56(1), 3–10. <https://doi.org/10.1088/1755-1315/56/1/012005>
- Soares, A. P. (2013). Arsip dan Manajemen Bencana di NEgeri Cincin Api. *Journal of Chemical Information and Modeling*, 53(9), 1689–1699.
- Suharmanto, P., Fitria, A. N., & Ghaliyah, S. (2015). Indonesian Geothermal Energy Potential as Source of Alternative Energy Power Plant. *KnE Energy*, 1(1), 119.

<https://doi.org/10.18502/ken.v1i1.325>

- Sutriani, W., & Wijayanto, B. (2020). Strategi Pengembangan Industri Energi Terbarukan Geothermal di Kabupaten Pasaman. *Geosee: Geography Science Education Explored Journal*, 1(1), 1–5.
- Umam, M. F., Muhammad, F., Adityama, D., & Purba, D. (2018). Tantangan Pengembangan Energi Panas Bumi Dalam Perannya terhadap Ketahanan Energi di Indonesia. *Swara Patra : Majalah Ilmiah PPSDM Migas*, 8(3), 48–65.
- Utama, G., Selama, L., Dan, T., Panjaitan, L. M., Fattah, E. I., Suhendi, C., Wulandari, R., & Perkasa, H. Y. (2020). *Analisis Pergerakan Dan Akumulasi Coulomb Stress*. 7(1), 35–39.
- Walter, T. R., Wang, R., Zimmer, M., Grosser, H., Lühr, B., & Ratdomopurbo, A. (2007). Volcanic activity influenced by tectonic earthquakes: Static and dynamic stress triggering at Mt. Merapi. *Geophysical Research Letters*, 34(5). <https://doi.org/10.1029/2006GL028710>
- Wells, Donald L. Coppersmith, K. J. (1994). *No New empirical relationships among magnitude, rupture length, rupture width, rupture area, and surface displacement*. Seismological Society of America, Berkeley, CA, United States. <https://doi.org/10.1785/BSSA0840040974>
- Wulandari, S., Parera, A. F. T., & Lubis, L. H. (2021). Relokasi Gempabumi di Sesar Renun A, B, Dan C dengan Menggunakan Metode Double Difference (Hypo-DD). *GRAVITASI: Jurnal ...*, 4. <https://ejournalunsam.id/index.php/JPFS/article/view/4560>